



HAL
open science

Oxidative C–N fusion of pyridinyl-substituted porphyrins

Mathieu Berthelot, Guillaume Hoffmann, Asmae Bousfiha, Julie Echaubard, Julien Roger, H el ene Cattey, Anthony Romieu, Dominique Lucas, Paul Fleurat-Lessard, Charles H. Devillers

► **To cite this version:**

Mathieu Berthelot, Guillaume Hoffmann, Asmae Bousfiha, Julie Echaubard, Julien Roger, et al.. Oxidative C–N fusion of pyridinyl-substituted porphyrins. *Chemical Communications*, 2018, 54 (43), pp.5414-5417. 10.1039/c8cc01375f. hal-02277741

HAL Id: hal-02277741

<https://hal.science/hal-02277741>

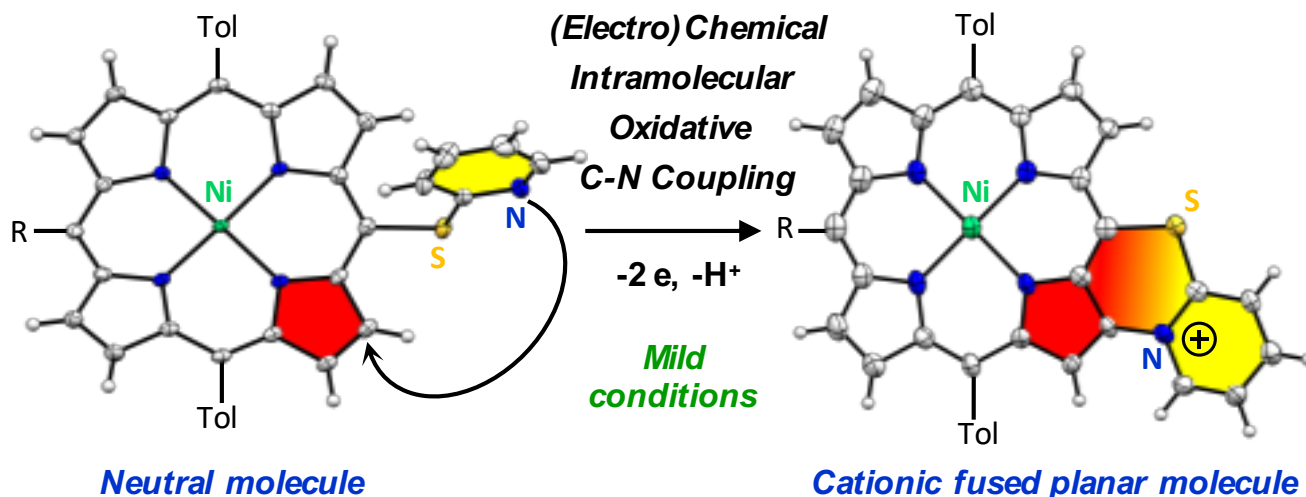
Submitted on 3 Sep 2019

HAL is a multi-disciplinary open access archive for the deposit and dissemination of scientific research documents, whether they are published or not. The documents may come from teaching and research institutions in France or abroad, or from public or private research centers.

L'archive ouverte pluridisciplinaire **HAL**, est destin ee au d ep ot et  a la diffusion de documents scientifiques de niveau recherche, publi es ou non,  emanant des  tablissements d'enseignement et de recherche fran ais ou  trangers, des laboratoires publics ou priv es.

Oxidative C-N Fusion of Pyridinyl-Substituted Porphyrins†

Mathieu Berthelot,^a Guillaume Hoffmann,^a Asmae Bousfiha,^a Julie Echaubard,^a Julien Roger,^a H el ene Cattey,^a Anthony Romieu,^{a,b} Dominique Lucas,^a Paul Fleurat-Lessard^a and Charles H. Devillers^{*a}

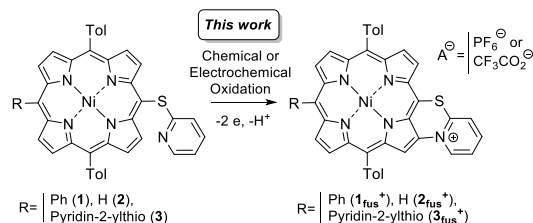


The mild (electro)chemical oxidation of pyridin-2-ylthio-*meso* substituted Ni(II) porphyrins affords C-N fused cationic and dicationic pyridinium-based derivatives. These porphyrins are fully characterized and the molecular structure of one of them was confirmed by X-ray crystallography. A mechanism for the intramolecular oxidative C-N coupling is proposed based on theoretical calculations and cyclic voltammetry analyses.

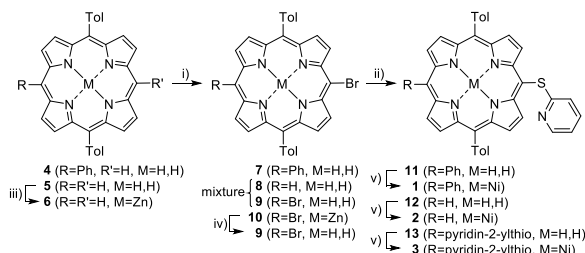
Over the last two decades π -extension of aromatic derivatives has attracted much attention because of potential applications in near-IR (NIR) electroluminescence displays, photovoltaic solar cells, non-linear optical materials, photodynamic therapy and molecular electronics.¹ The additional covalent C-C bond generated by the fusion reaction forces the aromatic core and the aromatic substituent to be coplanar which promotes enhanced electronic communication between both fragments. These π -extended molecules display important changes in their optical (bathochromic shift in their absorption/emission spectrum, large absorption and fluorescence in the NIR range, increase in the two-photon absorption cross section,...) and electrochemical (drastic decrease of the HOMO/LUMO gap) properties by comparison with the non-fused parent aromatic core.^{1b,2} In particular for porphyrins, "New efficient fusion reactions under milder conditions are highly desirable in future developments".³ For this purpose, "a better understanding of the mechanism of these intramolecular oxidative couplings is needed".⁴ Currently, these additional connections are produced by intramolecular C-C coupling using silver,⁵ iron,⁶ copper,⁷ palladium,^{6c,6d,8} scandium,^{2,9} gold¹⁰ and organic oxidants such as DDQ¹¹, PIDA,¹² PIFA¹²⁻¹³ often under relatively harsh conditions (chemical oxidizers in large excess,^{6d} high temperatures,¹⁴ acidic

medium¹⁵). These synthesized π -extended compounds are easier to oxidize than their starting unfused precursors due to the extended conjugation path. This feature could result in their over-oxidation/degradation, sometimes leading to low yield and/or poor air stability. Recently, two examples of mild electrochemically-driven intramolecular oxidative C-C coupling of *meso*-substituted-4,7-dimethoxynaphthalen-1-ylporphyrins have been reported.¹⁶ As demonstrated by the authors, the porphyrin cation radical was not sufficiently reactive to induce the C-C coupling. Formation of the porphyrin dication was necessary to promote the fusion reaction. At this applied potential, the fused product is oxidized to its reactive dication which may lead to further degradation. We reasoned that a peripheral substituent which might be able to generate a positive charge during the fusion reaction may allow to overcome this overoxidation issue. Pyridine is known to react in an intermolecular fashion with porphyrin cation radicals leading to pyridinium-porphyrin derivatives.¹⁷ These latter exhibit much higher oxidation potential (*ca.* from +100 to +300 mV) than the initial porphyrins accounting for the very good selectivity of the reaction.^{17a} To the best of our knowledge, only two examples of pyridine-based C-N intramolecular oxidative π -extension of an aromatic compound are reported. The first one described the electrochemical oxidative C-N fusion of a naphthol-substituted pyridine but the yield was only 4%.¹⁸ In the second example the electrochemically generated C-N benzene-based fused compounds were non-isolated intermediates.¹⁹ To our best knowledge, no example of C-N fused porphyrin synthesized by the direct intramolecular oxidative C-N fusion of a peripheral heterocyclic imine with a *meso* and/or β carbon from the porphyrin core is reported. (2-Pyridyl)thio was selected as the

peripheral *meso*-substituent to assess the feasibility of this reaction. Moreover, among the different metalloporphyrins, the Ni(II) complex was chosen since Ni(II) insertion makes the porphyrin more electrophilic, which should favor the C-N



Scheme 1 Intramolecular Oxidative C-N Fusion Reaction of Porphyrins 1-3.



Conditions: i) NBS, CHCl_3 , pyridine, 0 °C; ii) 2-mercaptopyridine, Cs_2CO_3 , DMF, 100 °C, Ar; iii) $\text{Zn}(\text{OAc})_2 \cdot 2\text{H}_2\text{O}$ (2 eq.), $\text{CHCl}_3/\text{MeOH}$, 60 °C; iv) TFA/ CH_2Cl_2 ; v) $\text{Ni}(\text{OAc})_2 \cdot 4\text{H}_2\text{O}$ (2 eq.), DMF, reflux, Ar.

Scheme 2 Synthesis of 1-3.

oxidative fusion reaction. To our delight, oxidation of porphyrins 1-3 gives for the first time, the C-N fused and positively charged pyridinium-porphyrins 1_{fus}^+ - 3_{fus}^+ (Scheme 1).

The synthesis of 1-3 is depicted in Scheme 2.[†] 7 and 8 were prepared by bromination of 5,15-bis(*p*-tolyl)-10-phenylporphyrin **4**²⁰ and 5,15-bis(*p*-tolyl)porphyrin **5**²⁰ with 1.2 and 0.8 eq. of NBS, respectively.²¹ To favor the monobrominated porphyrin **8**, a substoichiometric amount of NBS was used with **5**. In these conditions, a mixture containing **5** (28%), **8** (60%) and **9** (12%) was obtained. Exhaustive *meso*-dibromination of the porphyrin ring²² was not reached with the free base porphyrin **5**, even with an excess of NBS, but was achieved with the corresponding zinc(II) complex **6**,²³ leading quantitatively to the dibromoporphyrin **10**. Demetalation of **10** with TFA afforded the free base porphyrin **9**. The free base bromoporphyrins **7**, **8** and **9** were then functionalized with 2-mercaptopyridine *via* $S_N\text{Ar}$ reactions²⁴ providing porphyrins **11**, **12** and **13** in 78, 61 and 69% yield, respectively. In the last step, nickel(II) insertion leads to the complexes **1**, **2** and **3** in good yields.

1-3 have been characterized by NMR, HRMS, UV-vis absorption spectroscopy, cyclic voltammetry[†] and, for **1**[‡] and **2**,[§] by X-ray crystallography. In the ¹H NMR spectra (recorded in CDCl_3) of **1-3**, four pyridine-based multiplets appear between 5.80 and 8.45 ppm (Figures S16, S41 and S68). Due to the porphyrin proximity, these signals are shielded or unshielded as compared to the 2-mercaptopyridine molecule which displays four pyridine-based signals between 6.75 and 7.58 ppm.

The efficacy of the chemical oxidative coupling has been first evaluated on **1** in CH_2Cl_2 . Among the different tested oxidants (AgPF_6 , $\text{Fe}(\text{ClO}_4)_3$, DDQ/ $\text{Sc}(\text{OTf})_3$, PIFA and PIDA), PIFA gave satisfying results. Thus, oxidation of **1** with 1.2 eq. of PIFA at rt

produces 1_{fus}^+ , CF_3CO_2^- . To facilitate the purification process, CF_3CO_2^- anion was exchanged for PF_6^- using an anion exchange resin affording 1_{fus}^+ , PF_6^- in excellent yields (98%). Similar

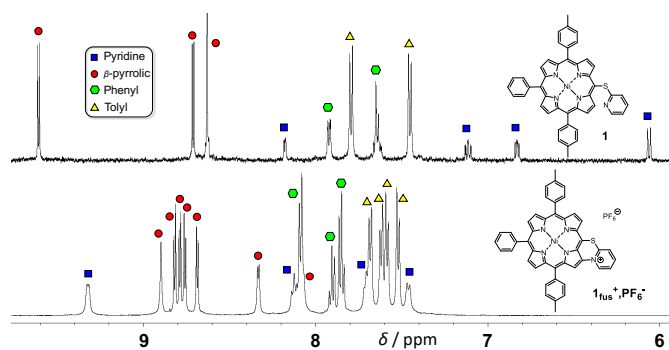
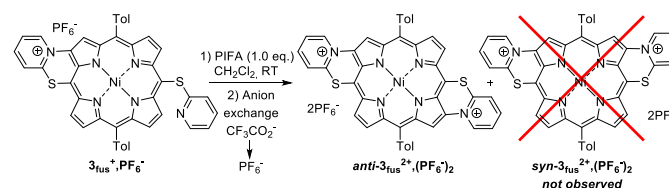


Figure 1 Partial ¹H NMR spectra of **1** and 1_{fus}^+ , PF_6^- (CD_3COCD_3 , 500 MHz, 300 K).



Scheme 3 Synthesis of $\text{anti-}3_{\text{fus}}^{2+},(\text{PF}_6^-)_2$

conditions were applied to **2** and **3**, providing 2_{fus}^+ , PF_6^- and 3_{fus}^+ , PF_6^- in 81 and 88 % yields respectively.[†] Oxidation of 3_{fus}^+ , PF_6^- with 1.0 eq. of PIFA leads to the doubly-fused dicationic compound $\text{anti-}3_{\text{fus}}^{2+},(\text{PF}_6^-)_2$, after anion exchange (31% yield). Remarkably, the reaction is perfectly regioselective as only the *anti* (3,13-fused) regioisomer was observed (Scheme 3). A similar regioselectivity has been previously reported when Ni(II) 5,15-bis(4-azulenyl)porphyrin was oxidized with FeCl_3 leading to the formation of two C-C bonds in an *anti*-configuration.^{9a} Theoretical study on the C-N bond formation revealed that the *anti* isomer is favored both kinetically and thermodynamically. Indeed, the SOMO of the cation radical of 3_{fus}^+ , PF_6^- presents a large coefficient on the *anti* β -position while no electronic density is observed on the *syn* β -position (Figure S102). Moreover, the *anti* isomer is also more stable than the *syn* one by 0.5 kcal mol⁻¹.

NMR (Figure 1 for 1_{fus}^+ , PF_6^-) and ESI-HRMS analyses confirm the molecular structure of the fused compounds.[†] In particular, the singlet integrating for one proton (two protons for $\text{anti-}3_{\text{fus}}^{2+},(\text{PF}_6^-)_2$) is assigned to the β -pyrrolic proton close to the position where the fusion takes place. Besides, due to loss of symmetry of the singly-fused molecules, the proton chemical shifts for the pyrrolic and tolyl fragments differ from each other. As a characteristic ¹H NMR feature of these singly-fused compounds, 1_{fus}^+ , PF_6^- exhibits two singlets integrating each one for 3 H at 2.73 and 2.69 ppm (in CD_3COCD_3) corresponding to the methyl fragments (Figure S23).

The molecular structure of 1_{fus}^+ , PF_6^- was definitively proven by X-ray diffraction analyses on monocrystals (Figure 2).^{§§} Comparing 1_{fus}^+ , PF_6^- and **1**, the formation of the new $\text{C}_\beta\text{-N}$ bond (1.423(5) Å) leads to a shorter $\text{C}_{\text{meso}}\text{-S}$ distance (1.744(5) vs. 1.772(3) Å) while the $\text{C}_{\text{meso}}\text{-S-C}_{\text{pyridine}}$ angle (105.4(2) vs. 103.02(13)°) increases. Each porphyrin interacts with two other

porphyrins by π -stacking (distance between two mean planes = 3.71 Å) leading to an infinite 1D network (Figure S99).

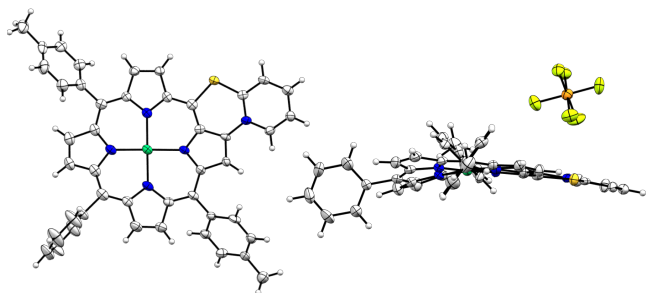


Figure 2 Front (left, PF_6^- anion omitted for clarity) and side (right) Mercury views of $\mathbf{1}_{\text{fus}}^+, \text{PF}_6^-$. Thermal ellipsoids are scaled to the 50% probability level.

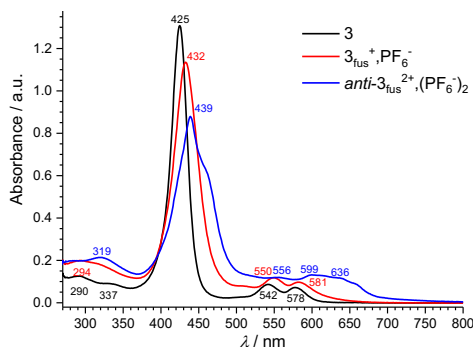


Figure 3 UV-vis. absorption spectra of $\mathbf{3}$, $\mathbf{3}_{\text{fus}}^+, \text{PF}_6^-$ and $\text{anti-}\mathbf{3}_{\text{fus}}^{2+}, (\text{PF}_6^-)_2$ in DMF ($C = 7.5 \times 10^{-6} \text{ M}$, $l = 1.00 \text{ cm}$).

As compared to $\mathbf{1-3}$, the UV-Vis. absorption spectra of the fused products[†] are red-shifted and a significant widening of the Soret bands is observed in agreement with the formation of π -extended porphyrins (see as an example Figure 3 for $\mathbf{3}$, $\mathbf{3}_{\text{fus}}^+, \text{PF}_6^-$ and $\text{anti-}\mathbf{3}_{\text{fus}}^{2+}, (\text{PF}_6^-)_2$).

$\mathbf{1-3}$ have been analyzed by cyclic voltammetry (CV). Contrary to what is commonly observed in CH_2Cl_2 for nickel(II) porphyrins,²⁵ the first oxidation peak of $\mathbf{1-3}$ (peak O1, Figure 4 for $\mathbf{1}$ and Figures S2 and S3 for $\mathbf{2}$ and $\mathbf{3}$ respectively) is fully irreversible which indicates that the electrogenerated porphyrin cation radical is not stable at the CV time scale. Reduction of the cation radical is only observed for scan rate higher than 100 V/s that gives an upper estimation of the half-life time of the cation radical ($t_{1/2} < 5 \text{ ms}$). This irreversible behavior indicates that $\mathbf{1}_{\text{fus}}^+ - \mathbf{3}_{\text{fus}}^+$ (with PF_6^- as the counter anion coming from the supporting electrolyte) are produced at the electrode surface during the CV analysis. For $\mathbf{1}$, the second and third oxidation systems (peaks O2/R2 and O3/R3, Figure 4) are fully reversible and are assigned to the oxidation of the fused compound $\mathbf{1}_{\text{fus}}^+, \text{PF}_6^-$ already formed at the electrode surface.

An exhaustive electrolysis at an applied potential corresponding to peak O1 was performed in presence of 2 equivalents of K_2CO_3 to avoid protonation and thus inactivation of the pyridine moiety during the electrolysis. After abstraction of *ca.* 2.5 Faradays, CV of the resulting solution revealed the disappearance of peak O1 in accordance with full consumption of $\mathbf{1}$ and the appearance of a new irreversible reduction peak (R6 at $E_{\text{pc}} = -0.77 \text{ V/SCE}$, Figure 4), which potential typically

corresponds to pyridinium reduction.^{17b} The reversible reduction peaks R7/O7 and R8/O8 are attributed to the

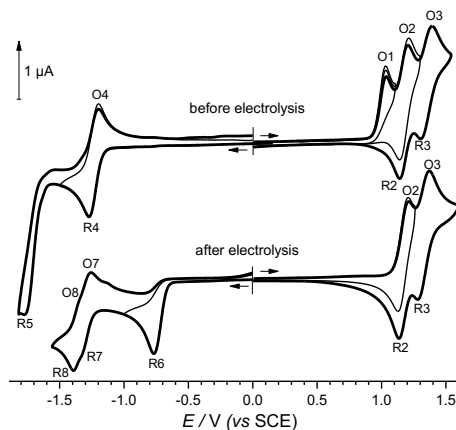
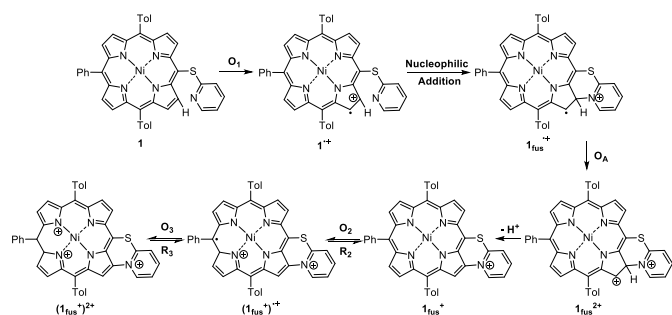


Figure 4 Cyclic voltammetry of a 10^{-3} M solution of $\mathbf{1}$ in CH_2Cl_2 0.1 M TBAPF_6 before (top) and after (bottom) electrolysis at $E_{\text{app}} = 0.96 \text{ V/SCE}$ (2.5 F), $v = 100 \text{ mV.s}^{-1}$, WE: Pt, $\varnothing = 1 \text{ mm}$.

reductions of the porphyrin ring leading to the radical anion and dianion. Interestingly, potentials and reversibility of peaks O2/R2 and O3/R3 remain unchanged before and after electrolysis. These observations corroborate the formation at the electrolysis time scale of the same product already observed during the CV analysis of $\mathbf{1}$. High resolution MALDI-TOF mass spectrometry analysis of the crude electrolyzed solution confirms the exclusive formation of $\mathbf{1}_{\text{fus}}^+$, with an m/z peak = 730.1559 (expected $m/z = 730.1570$ corresponding to the loss of one mass unit as compared to $\mathbf{1}$ for which $m/z = 731.1679$ (expected $m/z = 731.1654$). The electrogenerated fused compound was finally purified affording $\mathbf{1}_{\text{fus}}^+, \text{PF}_6^-$ in 71% isolated yield. Exhaustive electrolyses of $\mathbf{2}$ and $\mathbf{3}$ at the first oxidation potential in similar conditions also lead to the fused compounds $\mathbf{2}_{\text{fus}}^+, \text{PF}_6^-$ and $\mathbf{3}_{\text{fus}}^+, \text{PF}_6^-$ in 52 and 72% yields respectively. Synthesis of $\mathbf{3}_{\text{fus}}^{2+}, (\text{PF}_6^-)_2$ was achieved upon electrolysis of $\mathbf{3}_{\text{fus}}^+, \text{PF}_6^-$ in CH_3CN (23% yield).

When oxidized, $\mathbf{2}$ could follow two different pathways: 1) an intermolecular oxidative $C_{\text{meso}}-C_{\text{meso}}$ coupling^{5,26} and/or 2) an intramolecular oxidative $C_{\beta}-N_{\text{pyridine}}$ coupling, leading to the fused derivative. In our conditions, we did not notice any *meso-meso* dimer formation. The oxidation and C-N bond formation mechanisms have been theoretically investigated.[†] As for pyridine,^{17a} we confirmed that the C-N fusion of $\mathbf{1}$ occurs directly on the cation radical $\mathbf{1}^{\bullet+}$ (Scheme 4). It proceeds with a barrier of 12.8 kcal/mol corresponding to a half-life time of 0.3 ms, in fair agreement with the experimental upper limit $t_{1/2} < 5 \text{ ms}$. As expected,^{17a} oxidation of the fused cation radical occurs



Scheme 4 Oxidation and C-N fusion of 1.

at a lower potential than O1: $E_{pa}^{th}(O_A) = 0.96$ V vs. $E_{pa}^{th}(O_1) = 1.04$ V. O2 and O3 correspond to the oxidation of the fused compound. The oxidative fusion of 2 follows a similar route. When 3 is oxidized, 3_{fus}^+ will be formed first by following the same route as 1 (irreversible peak O1 in Figure S3). Then 3_{fus}^+ can be easily oxidized into a cation radical that will form the doubly fused *anti*- 3_{fus}^{2+} molecule that is then overoxidized. Oxidation of protonated fused radical cations are hidden as they occur at lower potentials than O1 and O2 respectively: $E_{pa}^{th}(O_A) = 1.05$ V (vs. $E_{pa}^{th}(O_1) = 1.13$ V) and $E_{pa}^{th}(O_B) = 1.22$ V (vs. $E_{pa}^{th}(O_2) = 1.25$ V).

In conclusion, three original Ni(II) pyridin-2-ylthio-*meso*-substituted porphyrins 1-3 have been synthesized and characterized. Their chemical and electrochemical oxidation performed in mild conditions (nearly stoichiometric amount of PIFA oxidizer, low oxidation potential, room temperature) leads, for the first time, to the formation of C-N fused pyridinium-based porphyrins. These unprecedented positively charged compounds are harder to oxidize than their precursors which allows to reach very good selectivity and fair to good yields for the fusion reaction. The ECEC mechanism proposed for the intramolecular C-N coupling is supported by theoretical calculations and voltammetric analyses. We want now to extend the scope of this efficient reaction to other peripheral substituents and porphyrin complexes and to explore the different applications of these porphyrin family newcomers.

This work is supported by the CNRS, Université de Bourgogne, Conseil Régional de Bourgogne through the "Plan d'Actions Régional pour l'Innovation (PARI)" and the "Fonds Européen de Développement Régional (FEDER)" programs. A.B. acknowledges the Ministère de l'Enseignement Supérieur et de la Recherche for a PhD grant. C. H. D. thanks the CNRS (Sept. 2015, one year "délégation CNRS") and the Agence Nationale de la Recherche for funding (ANR-15-CE29-0018-01). A. R. thanks the Institut Universitaire de France (IUF) for financial support. The authors are thankful to Dr. B. Habermeyer (PorphyChem Company) for generous gift of 5,15-ditylporphyrin sample, S. Fournier for technical support, M.-J. Penouilh for ESI-HRMS analyses. Calculations were performed using HPC resources from DSI-CCUB (Université de Bourgogne).

Conflicts of interest

There are no conflicts to declare.

Notes and references

‡‡ CCDC 1557313

§ CCDC 1557314

§§ CCDC 1813003

- (a) Y. Matsuo, Y. Sato, T. Niinomi, I. Soga, H. Tanaka and E. Nakamura, *J. Am. Chem. Soc.*, 2009, **131**, 16048; (b) J. D. Zimmerman, V. V. Diev, K. Hanson, R. R. Lunt, E. K. Yu, M. E. Thompson and S. R. Forrest, *Adv. Mater.*, 2010, **22**, 2780.
- N. K. S. Davis, A. L. Thompson and H. L. Anderson, *J. Am. Chem. Soc.*, 2011, **133**, 30.
- H. Mori, T. Tanaka and A. Osuka, *J. Mater. Chem. C*, 2013, **1**, 2500.
- J. P. Lewtak and D. T. Gryko, *Chem. Commun.*, 2012, **48**, 10069.
- A. Osuka and H. Shimidzu, *Angew. Chem., Int. Ed. Engl.*, 1997, **36**, 135.
- (a) M. Tanaka, S. Hayashi, S. Eu, T. Umeyama, Y. Matano and H. Imahori, *Chem. Commun.*, 2007, 2069; (b) J. P. Lewtak, D. Gryko, D. Bao, E. Sebai, O. Vakuliuk, M. Scigaj and D. T. Gryko, *Org. Biomol. Chem.*, 2011, **9**, 8178; (c) C.-M. Feng, Y.-Z. Zhu, S.-C. Zhang, Y. Zang and J.-Y. Zheng, *Org. Biomol. Chem.*, 2015, **13**, 2566; (d) N. Fukui, S.-K. Lee, K. Kato, D. Shimizu, T. Tanaka, S. Lee, H. Yorimitsu, D. Kim and A. Osuka, *Chem. Sci.*, 2016, **7**, 4059.
- B. J. Brennan, M. J. Kenney, P. A. Liddell, B. R. Cherry, J. Li, A. L. Moore, T. A. Moore and D. Gust, *Chem. Commun.*, 2011, **47**, 10034.
- S. Fox and R. W. Boyle, *Chem. Commun.*, 2004, 1322.
- (a) K. Kurotobi, K. S. Kim, S. B. Noh, D. Kim and A. Osuka, *Angew. Chem. Int. Ed.*, 2006, **45**, 3944; (b) H. Mori, T. Tanaka, S. Lee, J. M. Lim, D. Kim and A. Osuka, *J. Am. Chem. Soc.*, 2015, **137**, 2097; (c) A. Tsuda and A. Osuka, *Science*, 2001, **293**, 79.
- (a) A. K. Sahoo, Y. Nakamura, N. Aratani, K. S. Kim, S. B. Noh, H. Shinokubo, D. Kim and A. Osuka, *Org. Lett.*, 2006, **8**, 206; (b) K. Naoda, H. Mori, N. Aratani, B. S. Lee, D. Kim and A. Osuka, *Angew. Chem., Int. Ed.*, 2012, **51**, 9856.
- M. Pawlicki, K. Hurej, K. Kwiecinska, L. Sztterenberga and L. Latos-Grazynski, *Chem. Commun.*, 2015, **51**, 11362.
- L.-M. Jin, L. Chen, J.-J. Yin, C.-C. Guo and Q.-Y. Chen, *Eur. J. Org. Chem.*, 2005, 3994.
- (a) Q. Ouyang, Y.-Z. Zhu, C.-H. Zhang, K.-Q. Yan, Y.-C. Li and J.-Y. Zheng, *Org. Lett.*, 2009, **11**, 5266; (b) C.-M. Feng, Y.-Z. Zhu, Y. Zang, Y.-Z. Tong and J.-Y. Zheng, *Org. Biomol. Chem.*, 2014, **12**, 6990.
- V. V. Diev, C. W. Schlenker, K. Hanson, Q. Zhong, J. D. Zimmerman, S. R. Forrest and M. E. Thompson, *J. Org. Chem.*, 2012, **77**, 143.
- L. Barloy, D. Dolphin, D. Dupre and T. P. Wijesekera, *J. Org. Chem.*, 1994, **59**, 7976.
- (a) P. Chen, Y. Fang, K. M. Kadish, J. P. Lewtak, D. Koszelewski, A. Janiga and D. T. Gryko, *Inorg. Chem.*, 2013, **52**, 9532; (b) Y. Fang, D. Koszelewski, K. M. Kadish and D. T. Gryko, *Chem. Commun.*, 2014, **50**, 8864.
- (a) A. Giraudeau, L. Ruhlmann, L. El Kahef and M. Gross, *J. Am. Chem. Soc.*, 1996, **118**, 2969; (b) C. H. Devillers, A. K. D. Dimé, H. Cattey and D. Lucas, *Chem. Commun.*, 2011, **47**, 1893.
- G. Popp, *J. Org. Chem.*, 1972, **37**, 3058.
- T. Morofuji, A. Shimizu and J.-i. Yoshida, *Chem. Eur. J.*, 2015, **21**, 3211.
- C. H. Devillers, S. Hebié, D. Lucas, H. Cattey, S. Clément and S. Richeter, *J. Org. Chem.*, 2014, **79**, 6424.
- A. A. Ryan, S. Plunkett, A. Casey, T. McCabe and M. O. Senge, *Chem. Commun.*, 2014, **50**, 353.
- S. G. DiMagno, V. S. Y. Lin and M. J. Therien, *J. Org. Chem.*, 1993, **58**, 5983.
- H. A. Collins, M. Khurana, E. H. Moriyama, A. Mariampillai, E. Dahlstedt, M. Balaz, M. K. Kuimova, M. Drobizhev, V. X. D.

- Yang, D. Phillips, A. Rebane, B. C. Wilson and H. L. Anderson, *Nat. Photonics*, 2008, **2**, 420.
24. (a) Q. Chen, Y.-Z. Zhu, Q.-J. Fan, S.-C. Zhang and J.-Y. Zheng, *Org. Lett.*, 2014, **16**, 1590; (b) M. Kielmann, K. J. Flanagan, K. Norvaiša, D. Intrieri and M. O. Senge, *J. Org. Chem.*, 2017, **82**, 5122.
25. K. M. Kadish, E. V. Caemelbecke and G. Royal, in *The Porphyrin Handbook*, eds. K. M. Kadish, K. M. Smith and R. Guilard, Academic Press, 2000, vol. 8, pp. 1.
26. A. K. D. Dimé, C. H. Devillers, H. Cattet, B. Habermeyer and D. Lucas, *Dalton Trans.*, 2012, **41**, 929.